

First Structural Characterization of Neutral, Base-Stabilized Group 15-Pentaazides - Single Crystal X-ray Structures of dmap-As(N₃)₅ and dmap-Sb(N₃)₅

Benjamin Lyhs, Dieter Bläser, Christoph Wölper, Stephan Schulz^{*[a]}, Georg Jansen

Dedicated to Prof. Dr. H. Willner on the occasion of his 65th birthday

Institute of Inorganic Chemistry, University of Duisburg-Essen, Universitätsstr. 5-7, D-45117 Essen, Germany.

KEYWORDS. Covalent Azide - X-ray diffraction - DFT Computations.

Supporting Information Placeholder

ABSTRACT: Two neutral group 15-pentaazides dmap-As(N₃)₅ (**1**) and dmap-Sb(N₃)₅ (**2**) were synthesized and structurally characterized for the first time. Base-stabilization was confirmed to be very suitable for the kinetic stabilization of highly explosive covalent main group polyazides.

Introduction

Covalent main group element azides are long-known species in inorganic chemistry, but structural data were limited due to their expressed thermal and shock sensitivity.¹ In case of neutral binary group 15 triazides E(N₃)₃ (E = P, As, Sb, Bi),² only As(N₃)₃^{3a} and Sb(N₃)₃^{3a,3b} were structurally characterized by single crystal X-ray diffraction, to date. In contrast, from the corresponding binary pentaazides E(N₃)₅, whose lability toward dissociation into elemental nitrogen and the corresponding group 15 element is even more pronounced than that of the triazides, only As(N₃)₅ and Sb(N₃)₅ have been prepared,⁴ whereas P(N₃)₅⁵ and Bi(N₃)₅ are still unknown. Unfortunately, no neutral group 15 pentaazide was structurally characterized by single crystal X-ray diffraction, to date. The lack of structural data clearly results from their highly endothermic nature, according to which group 15 polyazides are not only of pure academic interest but are also interesting as high energy-density materials (HEDM).⁶ Many efforts have concentrated on the replacement of lead diazide, which is widely used as the primary explosive in propellants and explosives but unfortunately releases toxic lead into the environment, by alternate nontoxic energetic materials such as bismuth polyazides or other main group element polyazide.

The stability of covalent polyazides of group 15 elements can be increased by following two general procedures: addition or abstraction of additional azido groups which results in the formation of ionic species or addition of a Lewis base which yields the corresponding base-stabilized polyazides. In particular the ionic species are significantly less sensitive towards heat and shock. As a consequence, several trivalent polyazides including monocationic (E(N₃)₄⁺; P, As, Sb),⁷ monoanionic (E(N₃)₄⁻; As, Sb, Bi),^{2d,8,9} dianionic E(N₃)₅²⁻; Sb, Bi)^{8,9,10} and trianionic (Bi(N₃)₆³⁻)^{2d,9} polyazides as well as monoanionic hexaazides (E(N₃)₆⁻; P, As, Sb)^{5b,8,10,11} with the central group

15-atom in the formal oxidation state V have been synthesized and some (As(N₃)₄⁻,⁸ Sb(N₃)₄⁻,⁸ Bi(N₃)₄⁻,^{2d,9} Sb(N₃)₅²⁻,¹⁰ Bi(N₃)₅²⁻,^{8,9} Bi(N₃)₆³⁻,^{2d,9} P(N₃)₆⁻,^{11b} As(N₃)₆⁻,^{7c,11e} Sb(N₃)₆⁻,^{4,10} were structurally characterized by single crystal X-ray analysis. In contrast, single crystal X-ray analyses of base-stabilized neutral polyazides were only reported for the trivalent polyazides (py)₂Bi(N₃)₃,^{3b} bipyE(N₃)₃ (E = As, Sb)⁹ and [(bipy)₂Bi(N₃)₃]₂,⁹ whereas solid state structures of base-stabilized pentaazides are unknown, to date, even though Klapötke already synthesized a few of them 10 years ago.¹² Moreover, several base-stabilized group 13¹³ and group 14 polyazides¹⁴ have been synthesized and structurally characterized in the last decade.

Our general interest in the structural characterization of covalent main group element polyazides of group 15^{3b,10,15} and 17 elements¹⁶ directed our attention to the possible stabilization of neutral group 15 pentaazides of the type base-E(N₃)₅. Herein, we report on the synthesis and structural characterization of base-stabilized pentaazides dmap-E(N₃)₅ (E = As **1**, Sb **2**; dmap = 4-dimethylaminopyridine).

Experimental Section

General Procedures. Azidoarsenates and -antimonates are potentially toxic and can decompose explosively under various conditions! They should be handled only on a scale of less than 2 mmol with appropriate safety precautions (safety shields, safety glasses, face shields, leather gloves, protective clothing, such as leather suits, and ear plugs). Teflon containers should be used, whenever possible, to avoid hazardous fragmentation. Ignoring safety precautions can lead to serious injuries. Reactions were carried out in traps constructed from FEP tubes. Volatile materials were handled in a stainless steel-Teflon-FEP or Duran glass vacuum line, nonvolatile materials under Ar in a glove box. CH₂Cl₂ was dried over CaH₂ and degassed prior to use. (CH₃)₃SiN₃ was purified by fractional condensation and 4-dimethylaminopyridine (dmap) was sublimed prior to use. NMR spectra were recorded on a Bruker Avance 300 spectrometer at 25 °C at 300.1 MHz (¹H), 75.5 MHz (¹³C) and 21.7 MHz (¹⁴N). ¹H and ¹³C{¹H} NMR spectra were referenced to internal CDCl₃ (¹H: δ = 7.26; ¹³C: δ = 77.0) and ¹⁴N{¹H} spectra to external CH₃NO₂ (δ(¹⁴N) = 0). Raman spectra were recorded with a Bruker FT-Raman spectrometer RFS 100/S using the 1064 nm line of a Nd:YAG laser. The

backscattered (180°) radiation was sampled and analyzed (Stoke range: 0 to 3500 cm⁻¹). The powdered samples were measured in sealed capillaries (typical operation parameters: 4000 scans and a resolution of 2 cm⁻¹) using a laserpower of 80 mW. IR spectra were recorded on a Alpha-T FT-IR spectrometer with a single reflection ATR sampling module.

dmap-As(N₃)₅ (1). 2 mL of (CH₃)₃SiN₃ was condensed to 0.17 g (1 mmol) AsF₅ in a FEP reaction trap at -196 °C. The trap was slowly warmed to -60 °C over a period of 6 h, during which the mixture was occasionally (be careful!) agitated. 0.12 g (1 mmol) neat dmap was added at -60 °C and the reaction mixture was kept at -60 °C for 2 h and then slowly warmed to ambient temperature. Volatile components were pumped off, yielding a yellow solid residue. Yellow crystals of **1** were grown from a solution in CH₂Cl₂ by slow evaporation of the solvent in a dynamic vacuum.

Yield: 0.40 g (97 %). Melting point: 115 °C with gas evolution. IR (ATR, 32 scans): $\nu = 3313$ (w), 3134 (w), 3107 (w), 2502 (w), 2070 (s), 1624 (s), 1559 (s), 1521 (m), 1486 (w), 1438 (m), 1402 (m), 1344 (m), 1246 (s), 1225 (s), 1052 (s), 1016 (s), 944 (m), 813 (s), 670 (s), 571 (m), 518 (m), 426 (s) cm⁻¹. Raman (80 mW, 25 °C, 4000 scans): $\nu = 3105, 2938, 2869, 2822, 2111, 2094, 2081, 2069, 1631, 1564, 1315, 1269, 1052, 946, 817, 765, 717, 668, 431, 415, 303, 266, 224, 186, 105$ cm⁻¹. ¹H NMR (CDCl₃): $\delta = 3.23$ (s, 6H, N(CH₃)₂), 6.60 (m (AA'XX' spin system), 2H, H(3), H(5)), 8.47 (m, 2H, H(2), H(6)). ¹³C{¹H} NMR (CDCl₃): $\delta = 40.0$ (NMe₂), 105.3 (C(3), C(5)), 143.4 (C(2), C(6)), 156.1 (C(4)). ¹⁴N{¹H} NMR (CDCl₃): $\delta = -140$ (s, N_β, $\Delta\nu_{1/2} = 96$ Hz), -161 (s, N_γ, $\Delta\nu_{1/2} = 250$ Hz), -261 (s, N_α, $\Delta\nu_{1/2} = 980$ Hz).

dmap-Sb(N₃)₅ (2). 2 mL of (CH₃)₃SiN₃ was condensed to 0.22 g (1 mmol) SbF₅ in a FEP reaction trap at -196 °C. The trap was slowly warmed to -60 °C over a period of 6 h, during which the mixture was occasionally (be careful!) agitated. 0.12 g (1 mmol) neat dmap was added at -60 °C and the reaction mixture was kept at -60 °C for 2 h and then slowly warmed to ambient temperature. Volatile components were pumped off, yielding an off-white solid residue. Colorless crystals of **2** were grown from a solution in CH₂Cl₂ by slow evaporation of the solvent in a dynamic vacuum.

Yield: 0.45 g (98 %). Melting point: 104 °C with gas evolution. IR (ATR, 32 scans): $\nu = 3319$ (w), 2931 (w), 2490 (w), 2076 (s), 1647 (m), 1614 (s), 1558 (s), 1440 (m), 1400 (m), 1326 (m), 1252 (s), 1227 (s), 1213 (s), 1054 (m), 1000 (m), 943 (m), 810 (m), 660 (m), 578 (w), 514 (w), 416 (s) cm⁻¹. Raman (80 mW, 25 °C, 4000 scans): $\nu = 3099, 3027, 2935, 2868, 2822, 2120, 2086, 1628, 1560, 1421, 1312, 1276, 1253, 1228, 1055, 945, 764, 651, 417, 404, 239, 174, 100$ cm⁻¹. ¹H NMR (CDCl₃): $\delta = 3.24$ (s, 6H, N(CH₃)₂), 6.68 (m (AA'XX' spin system), 2H, H(3), H(5)), 8.32 (m, 2H, H(2), H(6)). ¹³C{¹H} NMR (CDCl₃): $\delta = 39.9$ (NMe₂), 106.6 (C(3), C(5)), 143.9 (C(2), C(6)), 156.4 (C(4)). ¹⁴N{¹H} NMR (CDCl₃): $\delta = -141$ (s, N_β, $\Delta\nu_{1/2} = 56$ Hz), -183 (s, N_γ, $\Delta\nu_{1/2} = 140$ Hz), -285 (s, N_α, $\Delta\nu_{1/2} = 930$ Hz).

Single Crystal Structure Determination of 1 and 2. Figures 2 and 3 show diagrams of the solid state structures of **1** and **2**. The crystals were mounted on nylon loops in inert oil. Data were collected on a AXS D8 Kappa diffractometer with APEX2 detector (MoK_α radiation, $\lambda = 0.71073$ Å; T = 100(1)

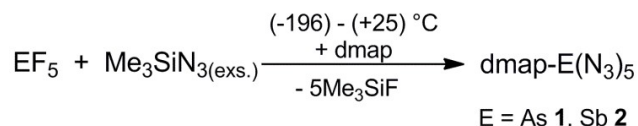
K). The structure was solved by Direct Methods (SHELXS-97)¹⁷ and refined by full-matrix least-squares on F². Absorption corrections were performed semi-empirically from equivalent reflections on basis of multi-scans (Bruker AXS APEX2). All non-hydrogen atoms were refined anisotropically, methyl hydrogen atoms as rigid groups and others by a riding model (SHELXL-97)¹⁸ **1**: [C₇H₁₀N₁₇As], M = 407.24, yellow crystal (0.45 x 0.38 x 0.12 mm); orthorhombic, space group *Pbca*; $a = 17.9789(5)$ Å, $b = 7.8016(2)$ Å, $c = 22.2904(6)$ Å; $\alpha = \beta = \gamma = 90^\circ$, $V = 3126.54(15)$ Å³, $Z = 8$; $\mu = 2.211$ mm⁻¹; $\rho_{\text{ber.}} = 1.730$ g cm⁻³; 86329 reflexes ($2\theta_{\text{max}} = 61^\circ$), 4732 unique ($R_{\text{int}} = 0.0428$); 226 parameters; largest max./min. in the final difference Fourier synthesis 0.527 eÅ⁻³ / -0.424 eÅ⁻³; max./min. transmission $0.75/0.43$; $R1 = 0.0273$ ($I > 2\sigma(I)$), $wR2$ (all data) = 0.0583. **2**: [C₇H₁₀N₁₇Sb], M = 454.07, colorless crystal (0.17 x 0.11 x 0.07 mm); monoclinic, space group *P2₁/c*; $a = 19.4550(5)$, $b = 14.0283(3)$, $c = 11.8465(3)$ Å; $\alpha = \gamma = 90^\circ$, $\beta = 90.0210(10)^\circ$, $V = 3233.215(14)$ Å³, $Z = 8$; $\mu = 1.742$ mm⁻¹; $\rho_{\text{ber.}} = 1.866$ g cm⁻³; 92119 reflexes ($2\theta_{\text{max}} = 61^\circ$), 9882 unique ($R_{\text{int}} = 0.0250$); 452 parameters; largest max./min. in the final difference Fourier synthesis 0.654 eÅ⁻³ / -0.356 eÅ⁻³; max./min. transmission $0.75/0.59$; $R1 = 0.0141$ ($I > 2\sigma(I)$), $wR2$ (all data) = 0.0362. The crystal was pseudomorphologically twinned by a rotation of 180° about *a*. As the metrics of the elemental cell suggested at first an orthorhombic lattice was assumed ($R_{\text{int}} = 12\%$), however systematic absences did not clearly lead to a space group. *Pbcn* was tried as it seemed most likely. The resulting solution could not be refined beyond an *R1* of 21.6% and an anisotropic refinement of the nitrogen and carbon atoms failed. The crystallographic data (without structure factors) were deposited as "supplementary publication no. CCDC-864145 (2) and CCDC-864146 (1)" at the Cambridge Crystallographic Data Centre. These data can be obtained free of charge from The Cambridge Crystallographic Data Centre: CCDC, 12 Union Road, Cambridge, CB21EZ (Fax: (+44)1223/336033; E-mail: deposit@ccdc.cam.ac.uk).

Computational calculation. All calculated molecular structures were fully geometry-optimized at the density functional theory (DFT) level, employing the B3LYP and BP86 exchange-correlation functionals.¹⁹ Except if denoted otherwise, no symmetry restrictions were applied. The Turbomole V6.0 quantum chemistry program package^{20,21} has been used in all of our calculations. The default criteria as found in Turbomole for convergence of the self-consistent field cycles and of the energy and the gradient during the geometry optimization procedure were tightened by one order of magnitude in each case. The grid size for numerical integration of the exchange-correlation functionals was improved to "m4" rather than the default "m3". A triple-zeta valence quality Gaussian type function basis set termed def2-TZVP²² has been used in all computations. The core electrons of the Sb atom were replaced with a scalar relativistic effective core potential.²³ While in the B3LYP calculations no further approximations were made, the resolution-of-the-identity approximation was employed in the BP86 computations, making use of an appropriate auxiliary basis set.²⁴ The BP86 level of theory has also been employed to verify that the optimized structures were minima on the molecular potential energy surface through computation of harmonic vibration frequencies from analytical second deriva-

tives.²⁵ Atomic partial charges were determined according to a natural population analysis (NPA).²⁶

Results and Discussion

Base-stabilized pentaazides $\text{dmap-E(N}_3)_5$ (E = As **1**, Sb **2**; $\text{dmap} = 4\text{-dimethylaminopyridine}$) were synthesized by reaction of equimolar amounts of freshly prepared samples of the pentaazides $\text{E(N}_3)_5$ (E = As, Sb) with dmap in Me_3SiN_3 . **1** and **2** were characterized by NMR (^1H , ^{13}C , ^{14}N), IR and Raman spectroscopy and by single crystal X-ray diffraction. The experimental structures agree well with those obtained from theoretical calculations *vide infra*.



Scheme 1. Synthesis of $\text{dmap-E(N}_3)_5$ (E = As **1**, Sb **2**).

^1H and ^{13}C spectra of **1** and **2** showed the expected resonances of the dmap base. ^{14}N NMR spectra (25 °C) of **1** and **2** each showed three well-resolved resonances due to the azido groups (**1**: -261, $\Delta\nu_{1/2} = 980$ Hz (N_α); -140, $\Delta\nu_{1/2} = 96$ Hz (N_β); -161 ppm, $\Delta\nu_{1/2} = 250$ Hz (N_γ); **2**: -285, $\Delta\nu_{1/2} = 930$ Hz (N_α); -141, $\Delta\nu_{1/2} = 56$ Hz (N_β); -183 ppm, $\Delta\nu_{1/2} = 140$ Hz (N_γ)), comparable to those observed for $\text{Sb(N}_3)_3$ (-321, $\Delta\nu_{1/2} = 170$ Hz (N_α); -134, $\Delta\nu_{1/2} = 26$ Hz (N_β); -169 ppm, $\Delta\nu_{1/2} = 34$ Hz (N_γ)) and other covalent azides.^{2c,3a} In contrast, the ^{14}N resonances of the dmap base were not observed.

Table 1. ^{14}N chemical shifts of $\text{dmap-E(N}_3)_5$ (E = As **1**, Sb **2**), $\text{E(N}_3)_3$ (E = As, Sb) and $\text{E(N}_3)_5$ (E = As, Sb).^[a]

Sample	N_α	N_β	N_γ	Ref.
$\text{As(N}_3)_3$ ^[b]	-318(15)	-131(15)	-165(30)	1a
$\text{Sb(N}_3)_3$ ^[c]	-321(170)	-134(26)	-169(34)	2b
$\text{As(N}_3)_5$ ^[d]	-282(v.br.)	-149(42)	-160(99)	3
$\text{Sb(N}_3)_5$	-	-	-	3
1 ^[b]	-261	-140	-161	this work
2 ^[b]	-285	-141	-183	this work
$\text{As(N}_3)_3$ ^[b]	-318(15)	-131(15)	-165(30)	1a

[a] In parenthesis $\Delta\nu_{1/2}$ values in Hz [b] CDCl_3 [c] CH_2Cl_2 [d] DMSO

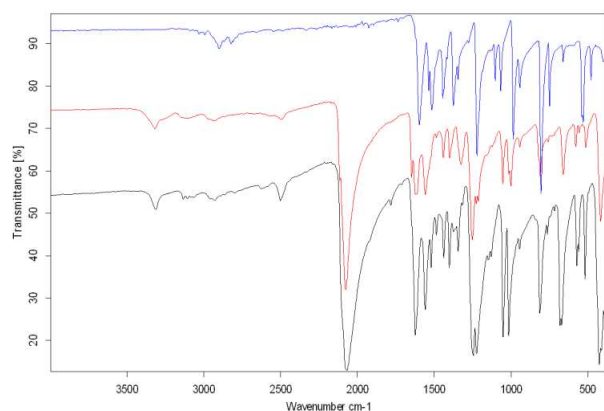


Figure 1. IR spectra of $\text{dmap-E(N}_3)_5$ (E = As **1**, Sb **2**) and dmap .

IR spectra of **1** and **2** (Fig. 1) show strong adsorption bands due to the asymmetric (**1**: $\nu = 2070$ cm^{-1} ; **2**: $\nu = 2076$ cm^{-1}) and symmetric N–N–N stretching mode (**1**: $\nu = 1246$ cm^{-1} ; **2**: $\nu = 1252$ cm^{-1}), which agree very well with calculated frequencies of the neutral, base-free pentaazides $\text{E(N}_3)_5$ and with values calculated by us at the BP86 level of theory *vide infra* (**1**: $\nu = 2130\text{-}2150$, 1280, 1290 cm^{-1} ; **2**: $\nu = 2121\text{-}2144$, 1281-1292 cm^{-1}). The N–N–N deformation modes (**1**: $\nu = 670$ cm^{-1} ; **2**: $\nu = 660$ cm^{-1}) also correspond well with reported values^[4] and with those calculated by us at the BP86 level of theory (**1**: $\nu = 652\text{-}671$ cm^{-1} ; **2**: $\nu = 634\text{-}652$ cm^{-1}).

Single crystals of **1** and **2** were obtained from solutions in CH_2Cl_2 by slow evacuation of the solvent. **1** crystallizes in the orthorhombic space group $Pbca$ whereas **2** crystallizes with two independent molecules in the monoclinic space group $P2_1/c$.

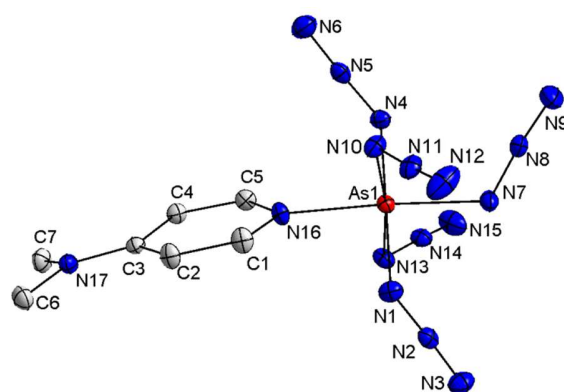


Figure 2. Representation of $\text{dmap-As(N}_3)_5$ **1** (hydrogen atoms omitted for clarity, thermal ellipsoids at 50% probability levels). Bond lengths [Å] and angles [°]: As1-N1 1.9233(13), As1-N4 1.9291(13), As1-N7 1.9348(13), As1-N10 1.9268(13), As1-N13 1.9238(12), As1-N16 1.9846(12), N1-N2 1.2338(18), N2-N3 1.1310(19), N7-N8 1.2290(18), N8-N9 1.1297(19); N1-As1-N4 179.59(6), N7-As1-N16 175.78(5), N13-As1-N10 172.97(5), N1-As1-N13 90.12(5), N1-As1-N10 90.32(6), N13-As1-N4 90.03(5), N10-As1-N4 89.48(6), N1-As1-N7 90.02(6), N13-As1-N7 90.14(6), N10-As1-N7 96.87(6), N4-As1-N7 90.36(6), N1-As1-N16 88.33(6), N13-As1-N16 85.98(5), N10-As1-N16 87.02(5), N4-As1-N16 91.31(5), N2-N1-As1 113.07(10), N14-N13-As1 115.76(10), N3-N2-N1 175.85(15), N9-N8-N7 174.89(16).

The N–N bond lengths within the azido ligands in **1** and **2** are in the typical range observed for covalent p-block azides. The differences between the $\text{N}_\alpha\text{-N}_\beta$ and $\text{N}_\beta\text{-N}_\gamma$ bond lengths, the latter are significantly shorter, clearly prove the covalent-bonded nature of the azido ligands. The azido ligands slightly deviate from linearity and show typical N–N–N bond angles of about 175°. The five E–N bond lengths toward the azido groups are almost equidistant (**1**: 1.9233(13) – 1.9348(13) Å; **2**: 2.0636(12) – 2.0814(12) Å) as was previously observed for hexaazidoarsenate and -antimonate ($[\text{E(N}_3)_6]^-$) anions (As–N 1.934(4) – 1.940(3),^{7c} 1.920(3) – 1.938(2) Å;^{11e} Sb–N 2.065(2) – 2.085(3),⁴ 2.0859(9) Å¹⁰). In remarkable contrast, the Sb–N bond lengths observed for the pentaazidoantimonite dianion ($[\text{Sb(N}_3)_5]^{2-}$) differ, with the equatorial Sb–N bond lengths (2.262(2) – 2.324(2) Å) significantly elongated compared to the axial Sb–N bond length (2.099(2) Å).¹⁰ Comparable struc-

tural findings were very recently reported for the pentaazido-bismutites $\text{Bi}(\text{N}_3)_5^{2-}$ dianions.^{8,9}

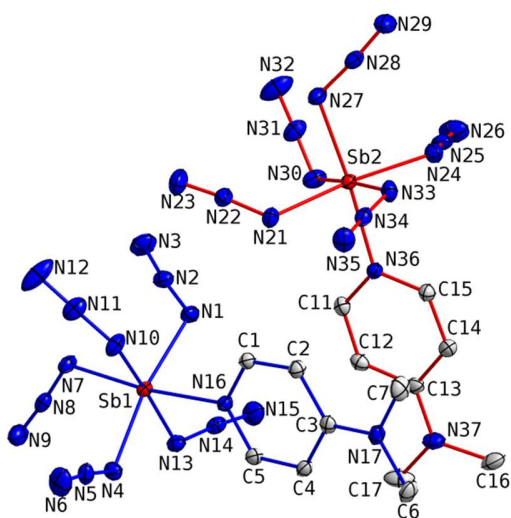


Figure 3. Asymmetric unit of $\text{dmap-Sb}(\text{N}_3)_5$, **2** consisting of two independent molecules (one depicted with red bond lines the other with blue ones; hydrogen atoms omitted for clarity, thermal ellipsoids at 50% probability levels). Bond lengths [Å] and angles [°] of one independent molecule (displayed with blue bonds): Sb1-N1 2.0814(12), Sb1-N4 2.0636(12), Sb1-N7 2.0716(12), Sb1-N10 2.0751(12), Sb1-N13 2.0726(13), Sb1-N16 2.1366(11), N1-N2 1.2311(19), N2-N3 1.1316(19), N7-N8 1.2255(18), N8-N9 1.1319(19), N1-Sb1-N4 170.25(5), N13-Sb1-N10 171.93(5), N7-Sb1-N16 172.95(5), N4-Sb1-N7 95.64(5), N4-Sb1-N13 79.79(5), N7-Sb1-N13 95.16(5), N4-Sb1-N10 93.63(5), N7-Sb1-N10 90.10(5), N7-Sb1-N1 91.73(5), N13-Sb1-N1 93.21(5), N10-Sb1-N1 92.74(5), N4-Sb1-N16 89.80(5), N13-Sb1-N16 90.21(5), N10-Sb1-N16 85.06(5), N1-Sb1-N16 83.40(5), Sb1-N1-N2 118.72(10), Sb1-N13-N14 119.67(10), N1-N2-N3 174.47(17), N7-N8-N9 175.68(15). The geometrical parameters of the second molecule are similar and can be found in the supporting material.

The As–N bond lengths of the covalently bound azido groups in **1** agree very well with the sum of the covalent radii as reported by Pyykkö et al. (1.92 Å)²⁷ as well as with the As–N bond lengths observed for neutral $\text{As}(\text{N}_3)_3$ (1.896(2) – 1.910(2) Å),^{3a} whereas those of the base-stabilized compound $\text{bipy-As}(\text{N}_3)_3$ (1.8823(13) – 1.9777(13) Å) is slightly elongated.⁹ The E–N $_{\alpha}$ bond lengths in $\text{bipy-As}(\text{N}_3)_3$ and $\text{bipy-Sb}(\text{N}_3)_3$, which can be described as strongly distorted pseudo-octahedrons, differ significantly. In both adducts, the shortest E–N $_{\alpha}$ bond lengths were found for the axial azido unit, whereas the equatorial ones are significantly elongated.⁹ The Sb–N bonds in **2** are slightly shorter than the sum of the covalent radii (2.11 Å).²⁷ Moreover, the Sb–N bond lengths observed for $\text{Sb}(\text{N}_3)_3$ (2.119(4) Å;^{3a} 2.119(5) – 2.151(5) Å)^{3b} and $\text{bipy-Sb}(\text{N}_3)_3$ (2.0783(9) – 2.2127(10) Å)⁹ are also elongated compared to those of **2**. The E–N $_{\text{dmap}}$ bond lengths in **1** and **2** (As1–N16: 1.9846(12) Å; Sb1–N16 2.1366(11) Å) are longer than the E–N $_{\text{azido}}$ bond lengths, clearly reflecting the donor-acceptor character.

The As and Sb atoms in **1** and **2** adopt only slightly distorted octahedral coordination geometries. Surprisingly, the four

equatorial azido groups are slightly bent toward the dmap molecule (N $_{\text{dmap}}$ –E–N 85.98(5)°–88.33(6)° (**1**), 83.40(5)°–89.80(5)° (**2**), exception N4–As1–N16 in **1** 91.31(5)° and N13–Sb1–N16 in **2** 90.21(5)°) This finding is rather unexpected since the dmap-base was expected to be sterically slightly more demanding than the axial azido group. On the other hand, the N $_{\text{dmap}}$ –E bond lengths in **1** and **2** are longer than the N $_{\alpha}$ –E bond lengths to the azido groups, hence diminishing the slightly bigger steric demand of the dmap base.

However in **1** three of the N $_{\text{dmap}}$ –As–N $_{\text{aeq}}$ –N $_{\text{beq}}$ absolute torsion angles are larger than 90° (123.43(11)°–136.67(12)°) and thus these equatorial azido ligands are oriented towards the axial one, away from the dmap. The azido group pointing towards the dmap (N16–As1–N4–N5 51.43(12)°) is generating a gap which is filled by the axial azido ligand (C1–N16 \cdots N7–N8 88.78(15)°). In each of the independent molecules of **2** the corresponding torsions are approx. 90° (72.46(12)°–87.38(12)°) for two of the azido groups and larger than 90° (125.54(12)°–175.56(12)°) for the two other ones. The axial azido ligands are oriented in a periplanar orientation towards the planes of the dmap rings (torsion about the N \cdots N vector: C1–N16 \cdots N7–N8 175.45(13)°, C11–N36 \cdots N27–N28 159.25(14)°). Since the N $_{\gamma}$ in **1** and **2** except for N6 and N26 in **2** are involved in – in some cases weak – non-classical hydrogen bonds the conformation of the molecules of is likely to be influenced by interionic interactions (*vide infra*, geometrical details see supporting material). A similar conformation influenced by CH \cdots N interactions was previously observed for the pentaazidoantimonite dianion ($[\text{Sb}(\text{N}_3)_5]^{2-}$)¹⁰ as well as for the corresponding dianionic pentaazidobismutites ($[\text{Bi}(\text{N}_3)_5]^{2-}$).^{8,9} In the latter case, however, packing effects on the conformation were not investigated. Apparently the intermolecular interactions in the packing of **1** only have minor impact on the conformation of the molecule. Although all N $_{\gamma}$ are accepting hydrogen bonds the general conformation differs only slightly from the one of the calculated structure (*vide infra*) and is qualitatively the same. One of the strongest (judged by crystallographic parameters: C7–H7a \cdots N9[x, -y-1/2, z-1/2] d(H \cdots A) 2.68 Å, $\angle(\text{NHA})$ 172.3°) only changes the C1–N16 \cdots N7–N8 torsion about 15°. The general structure is dominated by layers parallel to (001). Packing diagrams can be found in the supporting material.

In the packing of **2** the CH \cdots N bonds emanating from the pyridyl-group hydrogen atoms connect both molecules of the asymmetric unit and their symmetry equivalents generated by inversion thus forming an infinite chain parallel to the a-axis (see figure 4). The hydrogen bonds between the inverse molecules (C4–H4 \cdots N9[-x, -y+1, -z+1] d(H \cdots A) 2.49 Å $\angle(\text{NHA})$ 160.9°, C14–H14 \cdots N29[-x+1, -y+1, -z+1] d(H \cdots A) 2.64 Å $\angle(\text{NHA})$ 149.9°) are only possible because of the periplanar orientation of the axial azido group and the pyridyl ring. Consequently the conformation of the molecule can be considered to be distinctly influenced by intermolecular interactions since the observed C–N $_{\text{dmap}}$ \cdots N $_{\text{ax}}$ –N $_{\text{bx}}$ torsions are smaller than the one calculated to be energetically favored. Not surprisingly C4–H4 \cdots N9 alters the torsion more since it is the stronger one according to crystallographic parameters. The change in the torsion of the axial azido group influences - by sterical means - also the conformation of the equatorial azido groups.

The hydrogen atoms of the methyl groups link the chains by the formation of non-classical hydrogen bonds via *c*-glide plane symmetry and translation parallel to *c* resulting in a 3-dimensional network.

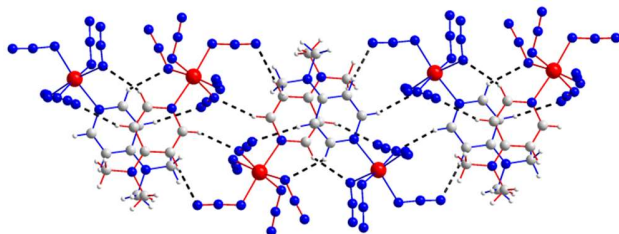


Figure 4. Chain formation parallel to *a* axis via $\text{CH}\cdots\text{N}$ in the packing of **2**. The bonds of the independent molecules of the asymmetric unit are displayed in different colours (red, blue), hydrogen bond in dashed lines.

Using the crystal structure parameters of **1** and **2** geometry optimizations with density functional theory (DFT) were carried out, employing the B3LYP and BP86 exchange-correlation functionals, a triple-zeta valence quality basis set and a relativistic pseudopotential for Sb. With both functionals the theoretical gas phase molecular structures did not show qualitative changes with respect to the crystal structure. The most significant bond length changes were observed for the As1-N16 bond, which is found to be 0.12 Å longer than in the crystal structure, and for Sb1-N16, which is about 0.11 Å longer. The other As-N bond lengths in **1** deviate between +0.00 and +0.02 Å at the B3LYP level and between +0.02 and +0.04 Å with BP86. The corresponding deviations for the remaining Sb-N bonds in **2** are +0.02 to +0.03 Å with B3LYP and +0.04 to +0.05 Å with BP86.

The N-N bond lengths in the azido groups agree within 0.02 Å between theory and experiment, the N-N-N bond angles within 1°. Larger deviations of up to 5° are found for the the N-As-N and N-Sb-N bond angles. We believe that the influence of the crystal structure environment is responsible for a major part of the deviations. Both levels of theory agree within 0.5° for the corresponding bond angles in **1** and within 1.5° for **2**.

The inclination of the four equatorial azido groups towards the dmap-base is also observed in the theoretical structures. In **1** the corresponding $\text{N}_{\text{ax}}\text{-As1-N16}$ angles vary between 84.9 and 88.6° at both levels of theory and the $\text{N}_{\text{ax}}\text{-Sb1-N16}$ angles in **2** between 82.2 and 87.8°. This can be attributed to repulsion between the partial charges on the N_{α} atoms, which according to a natural population analysis (NPA) with B3LYP in **1** amount to about -0.62 *e* on average for the azido ligands, while for N(16) only -0.52 *e* are found (with BP86 the corresponding values are -0.57 *e* and -0.49 *e*, respectively). In line with the fact that the positive partial charge on the Sb atom in **2** with 2.31 *e* (2.17 *e* with BP86) is larger than that of 2.08 *e* (1.96 *e* with BP86) on the As atom in **1**, we also note that the magnitude of the charges on the N_{α} atoms in **2** is larger: -0.64 *e* (-0.58 *e* with BP86) on average for the azido ligands and -0.54 *e* (-0.51 *e*) on N16. The increased repulsion between the N_{α} atoms thus is responsible for the somewhat stronger incli-

nation of the azido groups towards the dmap base in **2** as compared to **1**.

Since the structures of **1** and **2** show different arrangements of the azido groups, it is interesting to see which of the two structures would be lower in energy in the isolated molecule. We thus carried out geometry optimizations replacing the As atom in **1** with Sb and the Sb atom in **2** with As. Thus for **1** it was found that the optimized structure corresponding to that of **2** is 4.53 kJ/mol higher (3.47 kJ/mol with BP86) in energy, but nevertheless a local minimum structure according to a vibrational frequency analysis carried out at the BP86 level of theory. Also for **2** the optimized structure corresponding to that of **1** was found to be lower in energy, by 2.27 kJ/mol on the B3LYP level of theory (and by 1.14 kJ/mol with BP86). Thus, despite being a local minimum structure, the structure of **2** as found in the crystal is not the global minimum structure for an isolated monomer. The calculated energy differences are so small, however, that they may easily be overcome by interactions with neighboring molecules leading to optimal packing in the crystal.

Finally, since the observed and calculated structures of **2** are not far from displaying mirror symmetry, we also optimized **2** with C_s symmetry constraints. This led to a structure which is higher in energy by 0.35 kJ/mol at the B3LYP level of theory and only by 0.02 kJ/mol higher in energy with BP86. A frequency analysis at the BP86 level of theory shows that this structure corresponds to a first-order saddle point linking two C_1 -symmetrical enantiomers of **2**.

Conclusion. dmap- $\text{E}(\text{N}_3)_5$ (*E* = As, Sb) represent the first structurally characterized neutral group 15-pentaazides. Coordination of the strong Lewis-base dmap was found to be very effective for the kinetic stabilization of the highly explosive covalent group 15 pentaazides $\text{E}(\text{N}_3)_5$.

ASSOCIATED CONTENT

Supporting Information. Additional IR and Raman spectra of **1** and **2**, CIF files giving crystallographic data for complexes **1** and **2** as well as details on the computational calculations are given in the Supporting Information File. This material is available free of charge via the Internet at <http://pubs.acs.org>.

AUTHOR INFORMATION

Corresponding Author

* To whom correspondence should be addressed. E-Mail: stephan.schulz@uni-due.de.

Author Contributions

All authors have given approval to the final version of the manuscript.

ACKNOWLEDGMENT

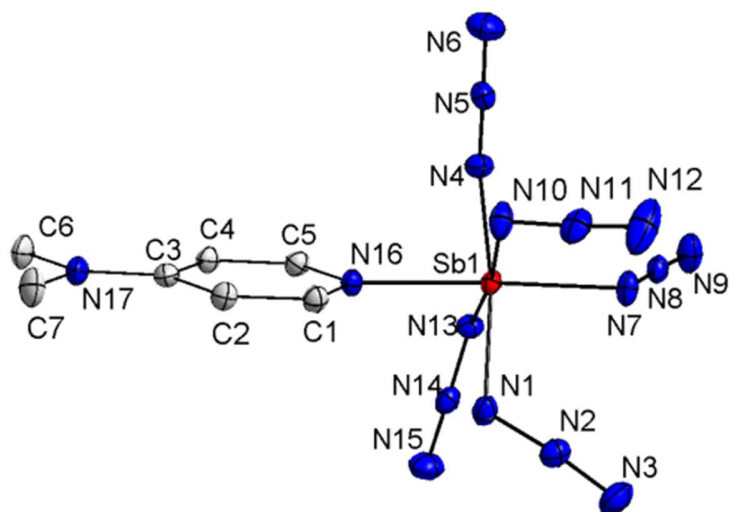
Stephan Schulz gratefully acknowledges financial support by the University of Duisburg-Essen.

ABBREVIATIONS

bipy, bipyridine; dmap, 4-dimethylaminopyridine; HEDM, high energy-density materials; py, pyridine.

REFERENCES

- (1) a) Klapötke, T. M.; *Chem. Ber.* **1997**, *130*, 443; b) Tornieporth-Oetting, I. C.; Klapötke, T. M. *Angew. Chem.* **1995**, *107*, 559; *Angew. Chem. Int. Ed.* **1995**, *34*, 511.
- (2) a) T. M. Klapötke, P. Geissler, *Dalton Trans.* **1995**, 3365. b) P. Geissler, T. M. Klapötke, H.-J. Kroth, *Spectrochim. Acta Part A* **1995**, *51*, 1075. c) T. M. Klapötke, A. Schulz, J. McNamara, *Dalton Trans.* **1996**, 2985. d) A. Villinger, A. Schulz, *Angew. Chem.* **2010**, *122*, 8190; *Angew. Chem. Int. Ed.* **2010**, *49*, 8017. The synthesis of $P(N_3)_3$ was reported, but it was neither isolated nor structurally characterized, to date. e) W. Buder, A. Schmidt, *Z. Anorg. Allg. Chem.* **1975**, *415*, 263; f) K. B. Dillon, A. W. G. Platt, T. C. Waddington, *Inorg. Nucl. Chem. Lett.* **1978**, *14*, 511. However, its photoelectron spectrum was reported. g) X. Zeng, W. Wang, F. Liu, M. Ge, Z. Sun, D. Wang, *Eur. J. Inorg. Chem.* **2006**, 416.
- (3) a) R. Haiges, A. Vij, J. A. Boatz, S. Schneider, T. Schroer, M. Gerken, K. O. Christe, *Chem. Eur. J.* **2004**, *10*, 508; b) S. Schulz, B. Lyhs, G. Jansen, D. Bläser, C. Wölper, *Chem. Commun.* **2011**, *47*, 3401.
- (4) R. Haiges, J. A. Boatz, A. Vij, V. Vij, M. Gerken, S. Schneider, T. Schroer, M. Yousufuddin, K. O. Christe, *Angew. Chem.* **2004**, *116*, 6844; *Angew. Chem. Int. Ed.* **2004**, *43*, 6676.
- (5) $P(N_3)_3$, initially reported by Buder et al., was later shown by Volgnandt et al. to be the hexaazide monoanion $P(N_3)_6^-$: a) W. Buder, A. Schmidt, *Z. Anorg. Allg. Chem.* **1975**, *415*, 263; b) P. Volgnandt, A. Schmidt, *Z. Anorg. Allg. Chem.* **1976**, *425*, 189).
- (6) R. Haiges, J. A. Boatz, A. Vij, M. Gerken, S. Schneider, T. Schroer, K. O. Christe, *Angew. Chem.* **2003**, *115*, 6027; *Angew. Chem. Int. Ed.* **2003**, *42*, 5847. See also: Klapötke, T. M.; Krumm, B. (2010) Azide-containing high energy materials. In: Bräse, S.; Banert, K. (eds) *Organic azides*, Wiley, Chichester, pp 391–411 and references therein.
- (7) a) A. Schmidt, *Chem. Ber.* **1970**, *103*, 3923; b) W. Buder, A. Schmidt, *Chem. Ber.* **1973**, *106*, 3812; c) K. Karaghiosoff, T. M. Klapötke, B. Krumm, H. Nöth, T. Schmitt, M. Suter, *Inorg. Chem.* **2002**, *41*, 170.
- (8) A. Schulz, A. Villinger, *Chemistry - A Eur. J.* **2012**, *18*, 2902.
- (9) R. Haiges, M. Rahm, D. A. Dixon, E. B. Garner, III, K. O. Christe, *Inorg. Chem.* **2012**, *51*, 1127.
- (10) B. Lyhs, G. Jansen, D. Bläser, C. Wölper, S. Schulz, *Chem. Eur. J.* **2011**, *17*, 11394.
- (11) a) H. W. Roesky, *Angew. Chem.* **1967**, *79*, 651; *Angew. Chem. Int. Ed.* **1967**, *6*, 637; b) P. Portius, P. W. Fowler, H. Adams, T. Z. Todorova, *Inorg. Chem.* **2008**, *47*, 12004; c) R. Haiges, S. Schneider, T. Schroer, K. O. Christe, *Angew. Chem.* **2004**, *116*, 5027; *Angew. Chem., Int. Ed.* **2004**, *43*, 4919; d) R. P. Singh, R. D. Verma, D. T. Meshri, J. M. Shreeve, *Angew. Chem.* **2004**, *118*, 3664; *Angew. Chem., Int. Ed.* **2006**, *45*, 3584; e) T. M. Klapötke, H. Nöth, T. Schütt, M. Warchhold, *Angew. Chem.* **2000**, *112*, 2197; *Angew. Chem. Int. Ed.* **2000**, *39*, 2108; f) A. Schmidt, *Chem. Ber.* **1970**, *103*, 3923; g) W. Buder, A. Schmidt, *Chem. Ber.* **1973**, *106*, 3812.
- (12) Klapötke, T. M.; Schütt, T., *J. Fluor. Chem.* **2001**, *109*, 151-162.
- (13) See the following and references cited therein: Haiges, R.; Boatz, J. A.; Williams, J. M.; Christe, K. O. *Angew. Chem.* **2011**, *123*, 38; *Angew. Chem. Int. Ed.* **2011**, *50*, 38.
- (14) See the following and references cited therein: Portius, P.; Filippou, A. C.; Schnakenburg, G.; Davis, M.; Wehrstedt, K.-D. Neutral Lewis Base Adducts of Silicon Tetraazide, *Angew. Chem.* **2010**, *122*, 43; *Angew. Chem. Int. Ed.* **2010**, *49*, 43.
- (15) B. Lyhs, D. Bläser, C. Wölper, S. Schulz, *Chem. Eur. J.* **2011**, *17*, 4914.
- (16) B. Lyhs, D. Bläser, C. Wölper, S. Schulz, G. Jansen, *Angew. Chem.* **2012**, *124*, 2008-2013; *Angew. Chem. Int. Ed.* **2012**, *51*, 1970-1974.
- (17) Sheldrick, G. M. *Acta Crystallogr. Sect. A* **1990**, *46*, 467.
- (18) SHELXL-97, Program for Crystal Structure Refinement, G. M. Sheldrick, Universität Göttingen, 1997. See also: Sheldrick, G. M. *Acta Crystallogr. Sect. A* **2008**, *64*, 112.
- (19) a) Dirac, P. A. M. *Proc. Roy. Soc. (London) A* **1929**, *123*, 714; b) Slater, J. C. *Phys. Rev.* **1951**, *81*, 385; c) Vosko, S. Wilk, L. Nussair, *M. Can. J. Phys.* **1980**, *58*, 1200; d) Becke, A. D. *Phys. Rev. A* **1988**, *38*, 3098; e) Lee, C.; Yang, W.; Parr, R. G. *Phys. Rev. B* **1988**, *37*, 785; f) Becke, A. D. *J. Chem. Phys.* **1993**, *98*, 5648; g) Perdew, J. P.; *Phys. Rev. B* **1986**, *33*, 8822.
- (20) TURBOMOLE V6.0 2009, a development of University of Karlsruhe and Forschungszentrum Karlsruhe GmbH, 1989–2007, TURBOMOLE GmbH, since 2007; available from <http://www.turbomole.com>
- (21) a) Ahlrichs, R.; Bär, M.; Häser, M.; Horn, H.; Kölmel, C. *Chem. Phys. Lett.* **1989**, *162*, 165. (b) Treutler O.; Ahlrichs, R. *J. Chem. Phys.* **1995**, *102*, 346. (c) von Arnim, M.; Ahlrichs, R. *J. Chem. Phys.* **1999**, *111*, 183.
- (22) Weigend F.; Ahlrichs, R. *Phys. Chem. Chem. Phys.* **2005**, *7*, 3297.
- (23) Metz, B.; Stoll, H.; Dolg, M. *J. Chem. Phys.* **2000**, *113*, 2563.
- (24) Weigend, F. *Phys. Chem. Chem. Phys.* **2006**, *8*, 1057.
- (25) Deglmann, P. May, K. Furche, F. Ahlrichs, R. *Chem. Phys. Lett.* **2004**, *384*, 103.
- (26) a) Reed, A. E. Weinstock, R. B. Weinhold, F. *J. Chem. Phys.* **1985**, *83*, 735. (b) Reed, A. E. Curtis, L. A. Weinhold, F. *Chem. Rev.* **1988**, *88*, 899.
- (27) P. Pyykko, M. Atsumi, *Chem. Eur. J.* **2009**, *15*, 186.



Neutral pentaazides of group 15 elements (As, Sb) can be stabilized by coordination of the strong Lewis base 4-dimethylamino pyridine (dmap), allowing their structural characterization for the first time.

DuEPublico

Duisburg-Essen Publications online

UNIVERSITÄT
DUISBURG
ESSEN

Offen im Denken

ub | universitäts
bibliothek

This text is made available via DuEPublico, the institutional repository of the University of Duisburg-Essen. This version may eventually differ from another version distributed by a commercial publisher.

DOI: 10.1021/ic300523k

URN: urn:nbn:de:hbz:464-20201112-090807-8

This document is the **Accepted Manuscript** version of a Published Work that appeared in final form in: *Inorg. Chem.* 2012, 51, 10, 5897–5902, copyright © American Chemical Society after peer review and technical editing by the publisher.

To access the final edited and published work see: <https://doi.org/10.1021/ic300523k>

All rights reserved.